Applied Physics Express

LETTER

Temperature-dependent study of $GaAs_{1-x-y}N_xBi_y$ alloys for band-gap engineering: photoreflectance and $k \cdot p$ modeling

Applied Physics Express 13, 091005 (2020)
https://doi.org/10.35848/1882-0786/abb286

LETTER

Temperature-dependent study of $GaAs_{1-x-y}N_xBi_y$ alloys for band-gap engineering: photoreflectance and $k \cdot p$ modeling

Wiktor Żuraw[1], Wojciech M. Linhart[1*], Jordan Occena[2], Tim Jen[2], Jared. W. Mitchell[2], Rachel S. Goldman[2], and Robert Kudrawiec[1]

[1]Department of Semiconductor Materials Engineering, Faculty of Fundamental Problems of Technology, Wrocław University of Science and Technology, Wybrzeże Wyspiańskiego 27, 50-370 Wrocław, Poland
[2]Department of Materials Science and Engineering, University of Michigan, Ann Arbor, Michigan 48109-2136, United States of America

*E-mail: wojciech.linhart@pwr.edu.pl

Received July 30, 2020; revised August 19, 2020; accepted August 25, 2020; published online September 4, 2020

Photoreflectance measurements were performed for $GaAs_{1-x-y}N_xBi_y$ layers in the temperature range of 20–300 K. For each sample a transition related to the band-gap was observed, which red-shifts with increasing nitrogen and bismuth content. The temperature dependencies of the band-gap were fitted by the Varshni and Bose–Einstein formulas and simulated within the band anticrossing model of the interaction between the extended band states of the GaAs and the localized states associated with nitrogen and bismuth atoms. The reduction of the band-gap was found to be ~80–100 meV. © 2020 The Japan Society of Applied Physics

Supplementary material for this article is available online

In recent years, the interest in group III–V semiconductor compounds diluted with bismuth has particularly increased due to a significant reduction of the band-gap at a low concentration of bismuth.[1–4] The reduction of the band-gap is accompanied by an increase in the energy split between the top of the valence band and the spin–orbit band.[5,6] The increase of this energy may have a significant application, especially if it exceeds the value of the band-gap, due to the attenuation of processes causing losses in lasers.[7,8] It has been also suggested that III–V semiconductor compounds diluted with bismuth have a reduced temperature sensitivity of the band-gap compared to conventional materials.[3,9] However, such conclusions were based on photoluminescence (PL) measurements, which is an emission-like method and very sensitive to localized states, especially at low temperatures.[10,11] The recommended methods for investigating the temperature dependence of the band-gap are absorption-like methods, such as photoreflectance (PR), which allows studying the optical transitions between the delocalized states.[10]

Group III–V semiconductors diluted with bismuth are classified as highly mismatch alloys (HMAs), in which the standard approximation of the virtual crystal cannot be used to calculate, for example, the band-gap value. The same group also includes III–V compounds diluted with nitrogen, which for the same reasons as bismuth are equally attractive and are used in various devices such as lasers, detectors, high performance solar cells, and heterojunction bipolar transistors.[12,13] The essential difference between these compounds is different size of the nitrogen and bismuth atoms. These atoms also have a different effect on the band structure of the compound into which they are introduced. In III–V dilute nitrides, the band anticrossing model is used for the conduction band, in contrast to bismides.[14–20] Both the introduction of nitrogen and bismuth reduce the band-gap, however, nitrogen reduces the lattice constant, while the addition of bismuth increases it. These phenomena are important for the development of new material systems, particularly in band-gap engineering. For example, adding nitrogen and bismuth to GaAs material causes strain compensation, so that the lattice constant of GaAsNBi is matched to the GaAs substrate while reducing the band-gap. It has been found that the molar ratio of nitrogen to bismuth for GaAsNBi matching to GaAs should be equal to 0.59,[21] although a recent paper suggests a revised value of 0.61.[22]

The temperature dependence of the band-gap energy of semiconductors represents a basic material-specific property which is of substantial practical and also theoretical interest. It is well known that the band-gap of semiconductors decreases monotonically with increasing temperature due to dilation of the lattice constant and the temperature-dependent electron–phonon interaction.[23] The temperature dependence of the band-gap was studied many times in the case of dilute $GaAs_{1-x}N_x$ and dilute $GaAs_{1-x}Bi_x$, however, it has not been studied for dilute $GaAs_{1-x-y}N_xBi_y$ compounds. In this letter, we present investigations of optical properties of $GaAs_{1-x-y}N_xBi_y$ alloys, using photoreflectance spectroscopy in the 20–300 K temperature range. Additionally, the obtained temperature dependencies were compared with the results calculated using the band anticrossing model.

A series of $GaAs_{1-x-y}N_xBi_y$ layers were grown on GaAs substrates by molecular beam epitaxy (MBE) at the University of Michigan. For the growth process, Ga, As and Bi solid sources and radio frequency nitrogen plasma were used. In order to produce the layers with different nitrogen and bismuth contents, one series was made at a constant flow rate N_2 of 0.25 sccm (Bi beam pressure was changed from 0 to 1×10^{-7} Tr) and a second series at a constant Bi beam pressure of 5.7×10^{-7} Tr (N_2 flow was adjusted from 0.17 to 0.35 sccm). Bi and N content in the samples was determined using nuclear reaction analysis and Rutherford backscattering spectrometry techniques. More information about measured samples can be found in Refs. 13 and 22.

For PR measurements a "bright configuration" of the experimental setup was used.[24] Samples were mounted on a cold finger in a helium closed-cycle refrigerator. Measurements in the 20–300 K temperature range were provided by the programmable temperature controller. The probe beam was made by 150 W tungsten-halogen bulb, while the pump source was a 150 mW laser with 405 nm wavelength. The light reflected from the sample was dispersed in a single grating 0.55 m focal-length monochromator and then was collected by a thermoelectrically cooled InGaAs pin photodiode.

The calculations of the band structure and the temperature dependence of the band-gap were performed utilizing the 12×12 $\mathbf{k} \cdot \mathbf{p}$ Hamiltonian for the valence bands described by Alberi et al.[5] and the two-level band anticrossing model for the conduction band.[14] Additionally, it should be mentioned that the host GaAs conduction band, includes the Kane nonparabolicity, due to interactions with the light-hole, heavy-hole and split-off bands, described by the 4×4 $\mathbf{k} \cdot \mathbf{p}$ Hamiltonian introduced by Pidgeon and Brown.[25] In this combined model a VBAC interaction is included between localized Bi 6 p-like states and the host valence bands, while a conduction band anticrossing (CBAC) interaction is included between the host conduction band and resonant nitrogen level.

Figure 1 shows the calculated band structure close to the Γ point of GaAs and a $GaAs_{0.926}N_{0.018}Bi_{0.056}$ alloy to illustrate the Bi- and N-induced band-gap reduction based on the previous report.[22] The calculation was carried out under the assumption that the valence band edge moves according to the valence band anticrossing (VBAC) model and the conduction band minimum shifts according to the CBAC model.[5,14] Figure 1 also depicts the localized Bi 6*p*-like states at 0.4 eV below the GaAs VBM (valence band maximum), spin–orbit split energy for the bismuth $E_{Bi-SO} = 1.9$ eV below VBM of GaAs, and the resonant energy of nitrogen level $E_N = \sim 1.65$ eV above the top of the GaAs VBM. For the calculations, the strength of the interaction of nitrogen level with the conductivity band was found to be $V_{MN} = \sim 2.5$ eV, while the strength of the interaction of bismuth level with the valence bands was found to be $V_{MBi} = \sim 1.5$ eV.[5,26,27] It is important to note that usually the conduction band edge and the valence band edge do not follow the same temperature dependence. The temperature dependence of the conduction band edge is mainly determined by the thermal expansion of the lattice parameter while the temperature dependence of the valence band edge is mostly determined by the electron–phonon interaction.[28] The temperature shift of the individual bands of the host matrix are given by the $\Delta E_{CB}^{host} = 3\frac{\Delta a(T)}{a} a_c^{\Gamma}$ and $\Delta E_{VB}^{host} = \Delta E_g - \Delta E_{CB}^{host}$, where $\frac{\Delta a(T)}{a}$ is the temperature-induced relative change of the lattice constant (6.03×10^{-6} [1/K] for GaAs[28]), a_c^{Γ} is the conduction band deformation potential (-11 eV for GaAs[28]), ΔE_g is the temperature-induced shift of the band-gap.

Figure 2 shows the PR spectra and corresponding fits of three of $GaAs_{1-x-y}N_xBi_y$ samples measured at temperatures between 20 and 300 K. It can be clearly observed that the position of the E_0 resonance in the of $GaAs_{1-x-y}N_xBi_y$ layers moves towards lower energies and broadens as the temperature increases. In order to determine the energy of the band-gap and its broadening, the PR spectra were fitted using the Aspnes formula

$$\frac{\Delta R}{R}(E) = Re[Ae^{i\theta}(E - E_0 + i\Gamma)^{-m}], \quad (1)$$

where $\frac{\Delta R}{R}(E)$ is the energy dependence of the PR signal, A is an amplitude, E_0 is the energy of optical transition, Γ is the broadening parameter of the optical transition and θ is the phase of the line.[29] The parameter m depends on the character of the optical transition, and it is assumed to be 2.5 for spectra at higher temperatures which correspond to a band-to-band transition. At low temperatures the E_0 transition can be excitonic ($m = 2$) and changes to band-to-band as the temperature increases. Such behavior can be observed in GaN(In)As alloys where their homogeneity is good enough. In our case, the band-to-bands and excitonic contributions are difficult to resolve in PR spectra due to alloy inhomogeneities which cause a substantial broadening of PR resonances. Additionally, the compressive strain in epilayers should provide a splitting of heavy- and light-hole bands, and hence the band-gap transition can be composed of two resonances: one related to the heavy-hole transition and second related to

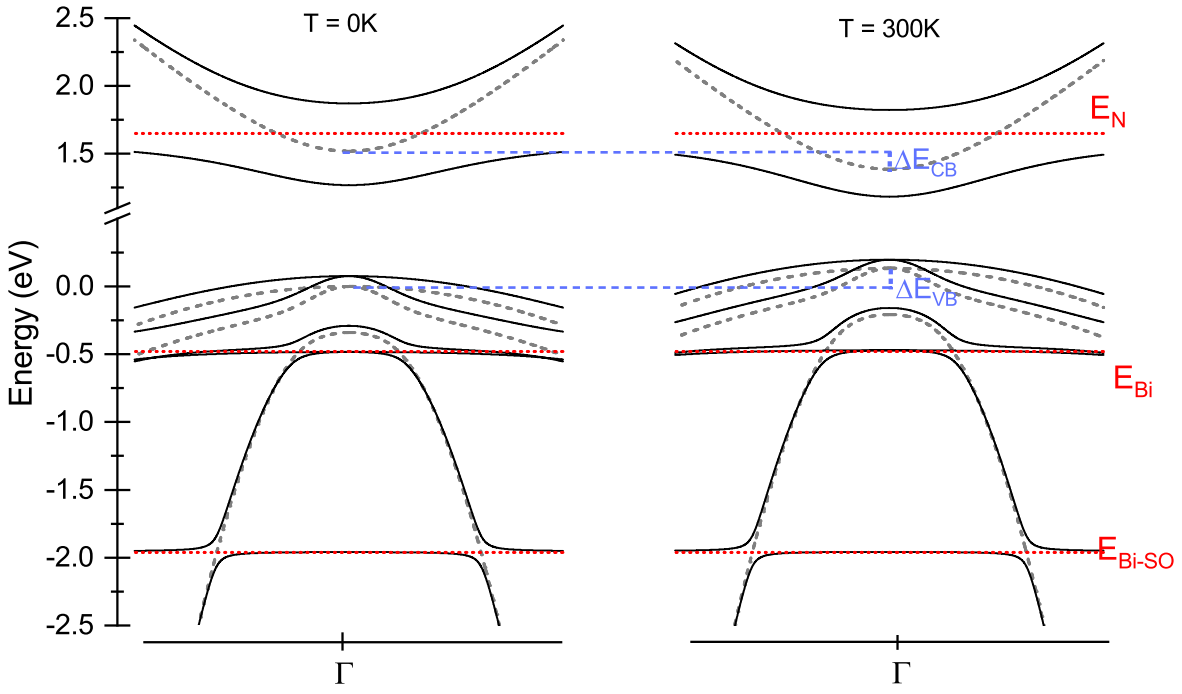

Fig. 1. (Color online) Band structure (solid black lines) near the center of Brillouin zone for $GaAs_{0.926}N_{0.014}Bi_{0.016}$ calculated using $k \cdot p$ model for 0 K and 300 K. The impurity levels of Bi and N are shown by the dotted line (red). The dashed (gray) line indicates the band structure of host GaAs. The solid lines indicate the bands after band anticrossing.

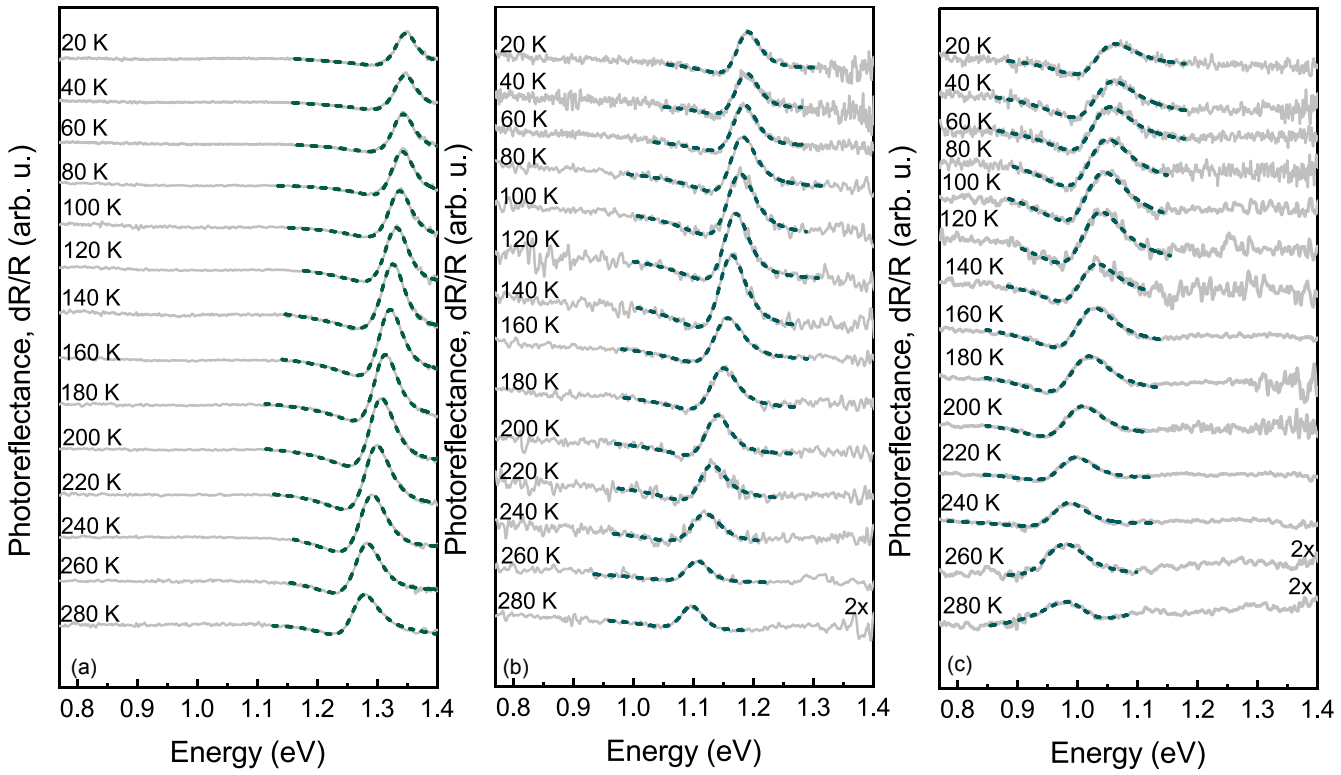

Fig. 2. (Color online) Temperature dependence of photoreflectance spectra of $GaAs_{1-x-y}N_xBi_y$ layers grown on GaAs. The dashed line shows the fit using Aspnes formula. (a) $x = 0.009$, $y = 0$, (b) $x = 0.014$, $y = 0.016$, (c) $x = 0.018$, $y = 0.030$.

light-hole transition.[30] This issue is more important for samples with larger Bi content. Our previous work on $GaAs_{1-x-y}N_xBi_y$ alloys has shown a PR resonance separation on heavy-hole transition and light-hole transition at the Γ point of the Brillouin zone.[22] However, in these investigations, the valence band splitting is neglected for all samples since the two resonances are not well resolved because of worse spectral resolution in this set of samples and also due to probing place on a sample, where inhomogeneity was possibly much greater causing large broadening and weak intensity of the light-hole related transition. For most samples the resonance amplitude becomes the highest for intermediate temperatures which may indicate the carrier localization at low temperatures. This results in a weaker modulation of the built-in electric field in the material and this is manifested by lower intensity of the PR signal.[31] It can be a confirmation of the thesis of localized states proposed in our previous work.[22]

Figures 3(a) and 3(b) show the temperature dependence of the band-gap extracted from the fitting procedure for all samples. It is clearly visible that the temperature-induced narrowing of the band-gap in $GaAs_{1-x-y}N_xBi_y$ alloys is significant in the range 20–300 K (∼82–95 meV) for the sample set with "constant" N and various Bi content [3(a)], and ∼66–99 meV for samples with "constant" Bi and various N content [3(b)]. These values are comparable with the value of GaAs of ∼88 meV.[32]

The temperature dependence of the band-gap has been fitted using both Varshni[23] and Bose–Einstein[33,34] formulas. The Varshni expression is given by

$$E_0(T) = E_0(0) - \frac{\alpha T^2}{\beta + T}, \tag{2}$$

where α and β are the so-called Varshni coefficients and $E_0(0)$ corresponds to the energy of optical transition at 0 K. The phenomenological Bose–Einstein relation, which takes into account the electron–phonon interaction is given by

$$E_0(T) = E_0(0) - \frac{2a_B}{\exp\left(\frac{\theta_B}{T}\right) - 1}, \tag{3}$$

where parameter a_B is related to the force of interaction between the electron and the phonon, and θ_B is the average temperature of phonon. The solid and dashed lines in Fig. 3 correspond to curves fitting the experimental data using Eqs. (2) and (3), correspondingly. The parameters obtained from the fittings are listed in the supplementary material, which is available online at stacks.iop.org/APEX/13/091005/mmedia. The obtained broadening parameter from PR spectra should be arranged according to Bose–Einstein relation

$$\Gamma_0(T) = \Gamma_0(0) - \frac{\Gamma_{LO}}{\exp\left(\frac{\theta_{LO}}{T}\right) - 1}, \tag{4}$$

where $\Gamma_0(0)$ is the value of broadening at 0 K resulting from the inhomogeneity of the sample content, Γ_{LO} is the constant of the electron coupling with an optical longitudinal phonon and θ_{LO} is the temperature of these phonons.[35]

Figures 3(c) and 3(d) depict the temperature dependence of the band edges calculated within the band anticrossing model (described in Fig. 1) for all investigated samples. It is visible that the temperature-dependent band-gap reduction is a result of the temperature shift of the bands, both the conduction band and the valence band. Mainly, it is caused by the shift of the individual bands of the host material (GaAs). However, after including the band anticrossing, bigger contribution into the band-gap reduction comes from the temperature shift of

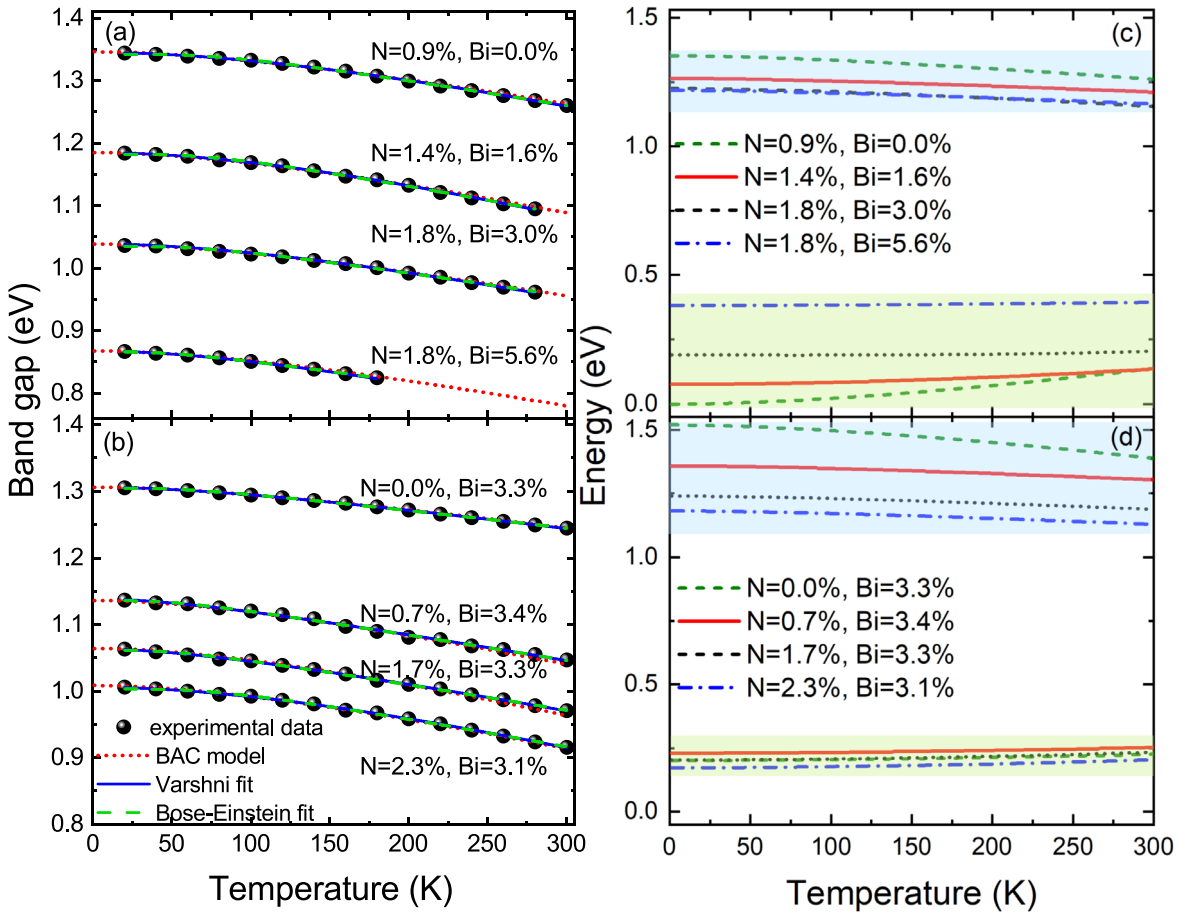

Fig. 3. (Color online) Temperature dependence of the band-gap for $GaAs_{1-x-y}N_xBi_y$ layers grown at (a) constant flow rate N_2 and (b) constant Bi beam pressure. The solid lines (blue) correspond to the Varshni fits—Eq. (2), the dashed lines (green) correspond to the Bose–Einstein fits—Eq. (3), while the dotted lines (red) show the theoretical temperature dependence of the band-gap resulting from the band anticrossing model. (c) and (d) Temperature dependence of particular band edge positions. Blue shaded regions denote the conduction band temperature evolution, whilst green shaded regions denote the valence band temperature evolution for each sample.

the conduction band; with increasing Bi content the temperature evolution of the valence band edge is getting less temperature sensitive. Similar analysis has been performed previously on GaNP, GaNPAs and N-rich GaNAs.[36,37]

It is important to note that in homogenous materials the broadening results from the intrinsic lifetime and other phenomena like alloy scattering. The temperature dependence of broadening parameter for an example sample is shown in Fig. 4. The value of the broadening at low temperatures for this sample is quite significant (~38 meV), which indicates large inhomogeneity. For the remaining samples, the broadening parameter was even higher due to increasing Bi content in the case of samples from the set with "constant" N content, or increasing N content in the case of samples with "constant" Bi content. This is shown in the inset of Fig. 4. Adding N and Bi into GaAs host results in the alloy content inhomogeneities and in appearing of the tail of density of states that in such alloy due to point defects, Bi pairs, N pairs, and other atom complexes.

For all measured samples the experimental data well correspond with the theoretical relation predicted by the band anticrossing model [see Figs. 3(a) and 3(b)]. For $GaAs_{0.926}N_{0.018}Bi_{0.056}$ the signal above 180 K could not be measured due to its low intensity. For materials containing nitrogen and bismuth, the difference between the band-gap in 20 K and 300 K was about 80–100 meV, while for a sample containing only bismuth ($GaAs_{0.967}Bi_{0.033}$) this value was visibly lower (~60 meV), which is also manifested in the lowest α coefficient for this sample, which was $(3.4 \pm 0.1) \times 10^{-4}$ eV K^{-1}. For comparison, the reduction of the band-gap in the range from 20 to 300 K for GaAs is about 100 meV and the α coefficient is equal to 5.4×10^{-4} eV K^{-1}.[38] Comparing the values of parameters a_B and θ_B, it can be concluded that for increasing nitrogen concentration the strength of interaction of electrons with phonons and the average temperature of phonons increases. In the case of bismuth impurity, this relation seems to be opposite—for materials with high bismuth to nitrogen ratio both parameters are significantly smaller compared to the rest of the samples.

The temperature dependence of the band-gap $GaAs_{1-x-y}N_xBi_y$ alloys has been studied using PR measurements and $k \cdot p$ modeling in the temperature range 20–300 K. In the obtained PR spectra one transition corresponding to the band-gap was observed. The obtained temperature dependencies were fitted by Varshni and Bose–Einstein relations and the experimental data have been well reproduced using the combined band anticrossing model. The reduction of the band-gap has been found to be ~80–100 meV, which is similar to

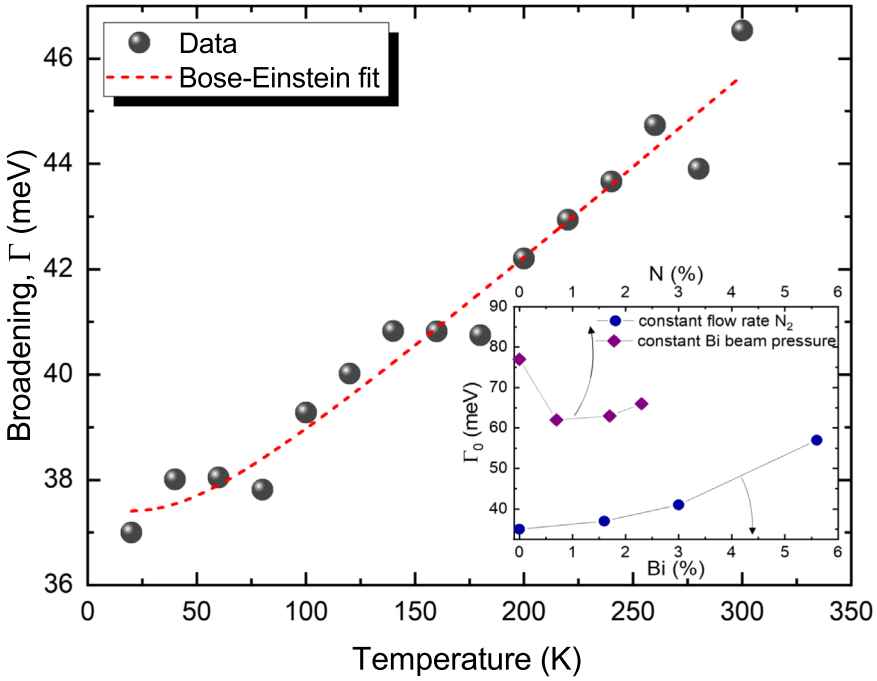

Fig. 4. (Color online) Temperature dependence of the broadening parameter for $GaAs_{0.97}N_{0.014}Bi_{0.016}$ layer with fit by the Bose–Einstein formula (red dashed line). Inset shows the broadening at 0 K as a function of Bi and N content.

GaAs. These results are important for band-gap engineering using GaAsNBi alloys and provide an insight into the combined influence of Bi and N on the electronic structure.

Acknowledgments We gratefully acknowledge support from the National Science Foundation (Grant Nos. DMR 1410282 and DMR 1810280) and the US Department of Energy Office of Science Graduate Student Research Program. Partial support is also provided by the Center for Integrated Nanotechnologies (CINT), a DOE nanoscience user facility jointly operated by Los Alamos and Sandia National Laboratories. W. M. Linhart acknowledges support from the Polish National Science Center Grant No. 2014/13/D/ST3/01947. This work was partly supported by a grant from the Ministry of Research and Innovation, CNCS-UEFISCDI, Project No. PN-III-P4-ID-PCE-2016-0742, within PNCDI III.

ORCID iDs Wojciech M. Linhart https://orcid.org/0000-0001-9879-6489

1) M. K. Rajpalke, W. M. Linhart, M. Birkett, K. M. Yu, D. O. Scanlon, J. Buckeridge, T. S. Jones, M. J. Ashwin, and T. D. Veal, Appl. Phys. Lett. **103**, 142106 (2013).
2) S. Tixier, M. Adamcyk, T. Tiedje, S. Francoeur, A. Mascarenhas, P. Wei, and F. Schiettekatte, Appl. Phys. Lett. **82**, 2245 (2003).
3) K. Oe and H. Okamoto, Jpn. J. Appl. Phys. **37**, L1283 (1998).
4) J. Kopaczek, R. Kudrawiec, W. M. Linhart, M. K. Rajpalke, K. M. Yu, T. S. Jones, M. J. Ashwin, J. Misiewicz, and T. D. Veal, Appl. Phys. Lett. **103**, 261907 (2013).
5) K. Alberi, J. Wu, W. Walukiewicz, K. M. Yu, O. D. Dubon, S. P. Watkins, C. X. Wang, X. Liu, Y. J. Cho, and J. Furdyna, Phys. Rev. B **75**, 045203 (2007).
6) Y. Zhong, P. B. Dongmo, J. P. Petropoulos, and J. M. O. Zide, Appl. Phys. Lett. **100**, 112110 (2012).
7) I. P. Marko and S. J. Sweeney, IEEE J. Sel. Top. Quantum Electron. **23**, 1501512 (2017).
8) P. Ludewig et al., Appl. Phys. Lett. **102**, 242115 (2013).
9) K. Oe and H. Asai, IEICE Trans. Electron. **E79-C**, 1751 (1996).
10) R. Kudrawiec and W. Walukiewicz, J. Appl. Phys. **126**, 141102 (2019).
11) R. Kudrawiec, M. Latkowska, M. Baranowski, J. Misiewicz, L. H. Li, and J. C. Harmand, Phys. Rev. B **88**, 125201 (2013).
12) A. Erol (ed.) *Dilute III–V Nitride Semiconductors and Material Systems* (Springer, Berlin, 2008).
13) J. Occena, T. Jen, E. E. Rizzi, T. M. Johnson, J. Horwath, Y. Q. Wang, and R. S. Goldman, Appl. Phys. Lett. **110**, 242102 (2017).
14) W. Shan, W. Walukiewicz, J. W. Ager, E. E. Haller, J. F. Geisz, D. J. Friedman, J. M. Olson, and S. R. Kurtz, Phys. Rev. Lett. **82**, 1221 (1999).
15) P. H. Jefferson, T. D. Veal, L. F. J. Piper, B. R. Bennett, C. F. McConville, B. N. Murdin, L. Buckle, G. W. Smith, and T. Ashley, Appl. Phys. Lett. **89**, 111921 (2006).
16) A. Lindsay and E. P. O'Reilly, Phys. Rev. Lett. **93**, 196402 (2004).
17) E. P. O'Reilly, A. Lindsay, P. J. Klar, A. Polimeni, and M. Capizzi, Semicond. Sci. Technol. **24**, 033001 (2009).
18) S. Fahy, A. Lindsay, H. Ouerdane, and E. P. O'Reilly, Phys. Rev. B **74**, 035203 (2006).
19) J. J. Mudd, N. J. Kybert, W. M. Linhart, L. Buckle, T. Ashley, P. D. C. King, T. S. Jones, M. J. Ashwin, and T. D. Veal, Appl. Phys. Lett. **103**, 042110 (2013).
20) W. M. Linhart, M. K. Rajpalke, J. Buckeridge, P. A. E. Murgatroyd, J. J. Bomphrey, J. Alaria, C. R. A. Catlow, D. O. Scanlon, M. J. Ashwin, and T. D. Veal T D, Appl. Phys. Lett. **109**, 132104 (2016).
21) A. Janotti, S. H. Wei, and S. B. Zhang, Phys. Rev. B **65**, 115203 (2002).
22) J. Occena, T. Jen, J. W. Mitchell, W. M. Linhart, E. M. Pavelescu, R. Kudrawiec, Y. Q. Wang, and R. S. Goldman, Appl. Phys. Lett. **115**, 082106 (2019).
23) Y. Varshni, Physica **34**, 149 (1967).
24) R. Kudrawiec and J. Misiewicz, Rev. Sci. Instrum. **80**, 096103 (2009).
25) C. R. Pidgeon and R. N. Brown, Phys. Rev. **146**, 575 (1966).
26) J. Wu, W. Shan, and W. Walukiewicz, Semicond. Sci. Technol. **17**, 860 (2002).
27) K. Alberi, O. D. Dubon, W. Walukiewicz, K. M. Yu, K. Bertulis, and A. Krotkus, Appl. Phys. Lett. **91**, 051909 (2007).
28) S. Adachi, *Elastic Properties, Properties of Semiconductor Alloys: Group-IV III–V II–VI Semiconductors* (Wiley, New York, 2009).
29) D. Aspnes, Surf. Sci. **37**, 418 (1973).
30) F. Dybała, J. Kopaczek, M. Gladysiewicz, E. M. Pavelescu, C. Romanitan, O. Ligor, A. Arnoult, C. Fontaine, and R. Kudrawiec, Appl. Phys. Lett. **111**, 192104 (2017).
31) R. Kudrawiec, G. Sek, J. Misiewicz, L. H. Li, and J. C. Harmand, Appl. Phys. Lett. **83**, 1379 (2003).
32) J. Yoshida, T. Kita, O. Wada, and K. Oe, Jpn. J. Appl. Phys. **42**, 371 (2003).
33) S. Logothetidis, L. Via, and M. Cardona, Phys. Rev. B **31**, 947 (1985).
34) P. Lautenschlager, M. Garriga, S. Logothetidis, and M. Cardona, Phys. Rev. B **35**, 9174 (1987).
35) P. Lautenschlager, P. B. Allen, and M. Cardona M, Phys. Rev. B **33**, 5501 (1986).
36) M. Wełna, K. Żelazna, A. Létoublon, C. Cornet, and R. Kudrawiec, Sol. Energy Mater. Sol. Cells **196**, 131 (2019).
37) E. Zdanowicz et al., Appl. Phys. Lett. **115**, 092106 (2019).
38) I. Vurgaftman, J. R. Meyer, and L. R. Ram-Mohan, J. Appl. Phys. **89**, 5815 (2001).